Formation, Localization, and Repair of L-Isoaspartyl Sites in Histones H2A and H2B in Nucleosomes from Rat Liver and Chicken Erythrocytes[†]

Wayne G. Carter[‡] and Dana W. Aswad*

Department of Molecular Biology and Biochemistry, University of California, Irvine, Irvine, California 92697

Received July 17, 2008; Revised Manuscript Received August 8, 2008

ABSTRACT: Formation of L-isoaspartyl (isoAsp) peptide bonds is a major source of protein damage *in vivo* and *in vitro*. Accumulation of isoAsp in cells is limited by a ubiquitous repair enzyme, protein L-isoaspartyl methyltransferase (PIMT). Reduction of PIMT activity in mouse brain or rat PC12 cells leads to a dramatic and selective accumulation of isoAsp sites in histone H2B. To learn more about the mechanism and specificity of isoAsp formation in histones, we purified mononucleosomes from rat liver and chicken erythrocytes and subjected them to *in vitro* aging for 0−16 days. In rat nucleosomes, the pattern of isoAsp accumulation duplicated that observed *in vivo*; only H2B accumulated significant isoAsp that we have now localized to the Asp25−Gly26 bond in the N-terminal tail. In chicken nucleosomes, isoAsp accumulated mainly in histone H2A and, to a lesser extent, in histone H2B. Minor sequence differences are consistent with the species-specific patterns of isoAsp accumulation and suggest that, in chicken, isoAsp occurs at the Asp121−Ser122 bond in the flexible C-terminal tail of H2A and at the Asp26−Lys27 bond in the N-terminal tail of H2B. The aging-induced accumulation of isoAsp in rat and chicken nucleosomes is repaired upon incubation of the damaged nucleosomes with PIMT and AdoMet. Our findings suggest that *in vivo* generation of isoAsp sites in histones occurs as a self-catalyzed process at the level of the nucleosome and is driven by the same structural features that have been shown to promote isoAsp formation in purified proteins and synthetic peptides.

Formation of L-isoaspartyl (isoAsp)[1]peptide bonds at aspartyl and asparaginyl residues constitutes a major source of spontaneous protein damage *in vitro* and *in vivo* (*1*−*6*). The level of isoAsp *in vivo* is normally kept low by the action of protein L-isoaspartyl methyltransferase (PIMT) (*7*−*9*). The reactions involved in the formation and repair of isoAsp are illustrated in Figure 1. To investigate the significance of isoAsp formation in cell function and its possible role in disease processes, we have sought to identify cellular proteins that are highly prone to isoAsp formation *in vivo*. This can be accomplished by reducing PIMT activity in living cells, followed by selective labeling of those proteins that accumulate isoAsp by ^{3}H-methylation of cell extracts with PIMT. Using pharmacological inhibition of PIMT in cultured rat PC12 cells, and a PIMT knockout mouse, we previously demonstrated that histone H2B is a major endogenous substrate for PIMT in the nucleus (*10*).

The structural determinants that promote isoAsp formation in proteins have been studied by *in vitro* aging of a variety of synthetic peptides and purified proteins (*5, 11*−*15*). These studies indicate that isoAsp formation is favored at Asn−X and Asp−X bonds when X is an amino acid with a small, hydrophilic side chain such as glycine or serine and when such sequence pairs fall in a flexible region of the polypeptide chain. While it is logical to assume that the same rules for isoAsp formation apply *in vivo*, there is little direct evidence to date to support this assumption.

Because histone modifications play a major role in gene regulation and cell division, we thought it would be informative to identify the sites of isoAsp formation that arise during *in vitro* aging of purified nucleosomes from two vertebrate species that have nonidentical histone sequences. Nucleosomes provide ample material for analysis while maintaining histones in a physiologically relevant context. We show here that the aging of rat liver nucleosomes gives rise to isoAsp formation primarily in histone H2B and that the rate of isoAsp formation is very similar to that which was previously estimated in PC12 cells cultured in the presence of a PIMT inhibitor. Peptide mapping of H2B from aged rat nucleosomes allowed us to establish Asp25-Gly26 in the N-terminal tail as the major site of isoAsp formation. In contrast, we found that isoAsp formation in aged chick nucleosomes occurs predominately in histone H2A. Sequence differences between rat and chicken somatic core histones are consistent with their differing patterns of isoAsp formation and suggest that the major isoAsp site in chicken H2A is at Asp121-Ser122 in the C-terminal tail. PIMT was able to repair essentially all of the isoAsp sites in rat and chicken nucleosomes.

[†] This work was supported by National Institutes of Health Grant NS17269 to D.W.A.

* To whom correspondence should be addressed. Tel: 949-824-6866. Fax: 949-824-8551. E-mail: dwaswad@uci.edu.

[‡] Present address: School of Biomedical Sciences, The University of Nottingham, Queen's Medical Centre, Nottingham NG7 2UH, U.K.

[1] Abbreviations: AdoHcy, *S*-adenosyl-L-homocysteine; AdoMet, *S*-adenosyl-L-methionine; isoAsp, isoaspartate or isoaspartyl; MALDI-TOF, matrix-assisted laser desorption ionization−time of flight; MES, 2-(*N*-morpholino)ethanesulfonic acid; PIMT, protein L-isoaspartyl methyltransferase; HPLC, high-performance liquid chromatography; PMSF, phenylmethanesulfonyl fluoride; TFA, trifluoroacetic acid; UAT (urea/acetic acid/Triton X-100).

10.1021/bi8013467 CCC: $40.75
Published on Web 09/17/2008

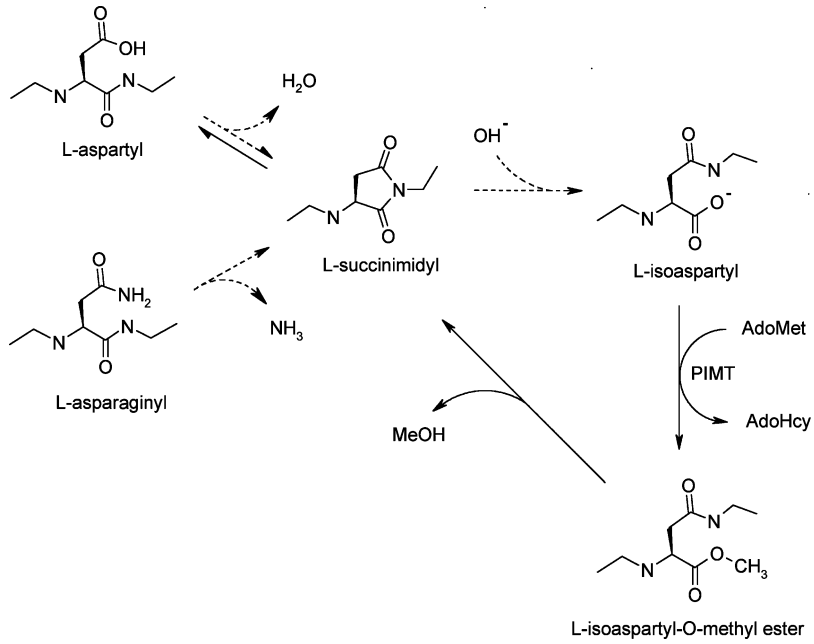

FIGURE 1: Mechanism of spontaneous isoaspartate formation and enzymatic repair in proteins. The formation of isoaspartyl sites (dashed arrows) starts with spontaneous dehydration of an Asp-Xaa linkage or deamidation of an Asn-Xaa linkage to produce a metastable succinimide that has a typical half-life of 2−4 h at physiological pH and temperature. The succinimide undergoes a spontaneous hydrolysis that generates an unequal mixture of two products; typically 15−30% of the product is a normal L-aspartyl linkage (solid arrow to upper left), with the remaining 70−85% going to form an abnormal L-isoaspartyl-Xaa linkage (dashed arrow to right). The isoaspartate repair pathway is indicated by the solid arrows. PIMT rapidly converts L-isoaspartyl sites to α-carboxyl-*O*-methyl esters (solid arrow down). At physiological pH and temperature, the α-carboxyl-*O*-methyl esters have a typical half-life of only a few minutes, undergoing spontaneous demethylation to re-form the same succinimide from which they originated. The final stage of repair occurs when a portion of the succinimide spontaneously hydrolyzes to generate a normal L-aspartyl site. Although the repair pathway requires multiple cycles for substantial net repair, its component reactions are rapid compared to the damage reactions that generate isoaspartyl sites; thus PIMT is able to maintain a very low steady-state level of isoaspartyl protein sites *in vivo*. The repair pathway shown here is also the basis for *in vitro* assays of isoaspartate levels in proteins. If [*methyl*-^{3}H]AdoMet is used as the methyl donor, isoaspartate levels in proteins can be quantitated by measuring [^{3}H]methyl incorporation into the protein of interest or by measuring the production of [^{3}H]methanol. IsoAsp content can also be determined using unlabeled AdoMet by measuring the stoichiometric production of AdoHcy from unlabeled AdoMet.

EXPERIMENTAL PROCEDURES

Materials. *S*-Adenosyl-L-methionine (AdoMet), *S*-adenosyl-L-homocysteine (AdoHcy), spermidine hydrochloride, spermine hydrochloride, and protamine were purchased from Sigma. S7 micrococcal nuclease, endoproteinase Glu-C, and 3,4-dichloroisocoumarin were purchased from Roche Molecular Biochemicals. *S*-Adenosyl-L-[*methyl*-^{3}H]methionine (15 Ci/mmol) was purchased from PerkinElmer-NEN. Where indicated, the specific activity was diluted by mixing with unlabeled AdoMet that had been purified by chromatography on (carboxymethyl)cellulose (*16*). The isoAsp-5 form of δ-sleep-inducing peptide (WAGGDSGE) was purchased from Bachem California. Homogeneous rat recombinant PIMT expressed in *Escherichia coli* was prepared as described by David and Aswad (*17*). PIMT is commercially available as part of the IsoQuant isoAsp analysis kit available from Promega, Inc.

Preparation of Nucleosomes from Rat Liver and Chicken Erythrocytes. Nuclei from rat liver and chicken erythrocytes were purified by the methods of Hewish and Burgoyne (*18*) and Weintraub et al. (*19*), respectively. These procedures are described in detail in protocol 1 (rat liver) and protocols 2 and 3 (chicken erythrocytes) of Thomas (*20*). Fresh livers were obtained from adult Sprague-Dawley rats that were euthanized with an overdose of Nembutal followed by decapitation, rapidly frozen, and stored at −70 °C until needed. Fresh chicken blood was obtained from a local commercial supplier and processed immediately. Nuclei were stored at −70 °C at a concentration of 5 mg/mL chromatin (A_{260} = 50) until needed.

Soluble chromatin was prepared from nuclei by S7 nuclease digestion according to protocol 8 of Thomas (*20*). Digestion conditions were adjusted to optimize the yield of mononucleosomes as judged by agarose gel electrophoresis. Final purification of mononucleosomes was achieved by subjecting the digested chromatin (2−3 mL, A_{260} = 25−30) to gel filtration at 4 °C on a 1.8 × 30 cm column of Sephadex G-150 superfine. The column was run at a flow rate of approximately 0.2 mL/min in 20 mM Tris-HCl, pH 7.5, 25 mM NaCl, 0.2 mM EDTA, 1 mM DTT, 0.25 mM PMSF, and 0.02% sodium azide. Absorbance of the effluent was monitored at 260 nm. The mononucleosome peak (containing ca. 5% dinucleosomes) eluted near the void volume. Diafiltration was used to concentrate the pooled peak fractions and to exchange them into "aging buffer" (50 mM K-HEPES, pH 7.4, 1 mM EGTA, 5% (w/v) glycerol, 1 mM DTT, 0.25 mM PMSF, 0.02% sodium azide). The nucleosomes were stored at −70 °C at a protein concentration of 2.1−3.1 mg/mL.

In Vitro Aging of Nucleosomes. Nucleosomes were diluted to a protein concentration of 2.0 mg/mL in aging buffer and incubated at 37 °C in closed microcentrifuge tubes for 16 days. Samples were removed at 4 day intervals and stored at −70 °C prior to analysis of isoAsp content.

Quantitation of IsoAsp Levels in Nucleosomes. The total isoAsp content of nucleosomes was determined by measuring the stoichiometric production of *S*-adenosyl-L-homocysteine (AdoHcy) that is generated when isoAsp-containing proteins or peptides are incubated with PIMT and an excess of AdoMet. The AdoHcy produced is separated from other reaction components by reversed-phase high-performance liquid chromatography (RP-HPLC) and quantitated by UV absorption at 258 nm relative to a standard. Details of this assay are described in Schurter and Aswad (*21*).

Radiolabeling of IsoAsp Sites by ^{3}H-Methylation. IsoAsp sites in nucleosomes, samples of histone H2B isolated from nucleosomes, or enzymatic digests of histone H2B were ^{3}H-methylated for 10 min at 30 °C in reactions (20−100 μL) consisting of 50 mM K-MES, pH 6.2, 3 μM PIMT, 0.2−0.5 μg/μL nucleosomal or histone protein, and 20 μM [*methyl*-^{3}H]AdoMet (10000 dpm/pmol). Reactions were terminated by addition of a stop solution (below) that varied with the type of subsequent analysis. (1) Reactions destined for analysis by polyacrylamide gel electrophoresis in sodium dodecyl sulfate (SDS−PAGE) were terminated by adding a $^1/_4$ volume of 5× SDS−PAGE sample buffer (*22*) followed by heating for 10 min at 50 °C. (2) For gel electrophoresis in urea/acetic acid/Triton X-100 (UAT), reactions were terminated by adding an equal volume of UAT loading buffer consisting of 8 M urea, 5% (v/v) acetic acid, 5% (v/v) 2-mercaptoethanol, 1.25 mg/mL protamine sulfate, and 0.02% (w/v) pyronin-Y. (3) For reversed-phase HPLC, reactions were terminated by adding trifluoroacetic acid (TFA) to a final concentration of 0.3% (v/v).

Gel Electrophoresis and Fluorography of ^{3}H-Methylated Nucleosomes. SDS−PAGE was carried out in 4−12% acrylamide NuPAGE Bis-Tris minigels using the MES running buffer (Invitrogen). To minimize the loss of labile protein methyl esters, electrophoresis was carried out at 100 V for 4 h in a 4 °C cold room using precooled running buffer (*23*). Proteins were stained with Coomassie Blue R-250, destained, photographed, and then subjected to fluorography by the salicylate method of Chamberlain (*24*).

UAT gels (10 cm × 10 cm × 0.75 mm) were cast and run in a manner similar to that described by Wiekowski and DePamphilis (*25*). A 1 cm high detergent-free plug gel, composed of 15% acrylamide/bisacrylamide (19:1), 8 M urea, and 5% (v/v) acetic acid (v/v), was first cast as a base to prevent main gel slippage during electrophoresis. Next, the polymerized base plug was overlaid with a main gel containing the same components plus 0.375% (w/v) Triton X-100. After polymerization of the main gel, the well comb was removed, and the sample wells were filled with a solution of 8 M urea, 5% (v/v) acetic acid, and 0.375% (w/v) Triton X-100. The gel was pre-run at 200 V, with upper chamber as anode (−), for 1 h at room temperature with 5% (v/v) acetic acid in the electrode chambers. After the sample wells were rinsed well with 5% (v/v) acetic acid, samples were loaded, and electrophoresis was carried out at 200 V for 2 h at room temperature with the upper chamber serving as the cathode (+). Gels were stained and subjected to fluorography as described above.

HPLC of ^{3}H-Methylated Nucleosomes. ^{3}H-Methylation reactions (stopped with TFA as described above) were loaded onto a 100 × 4.6 mm Brownlee RP-300 column equilibrated with 0.3% TFA in HPLC grade water. Sample loading and subsequent chromatography were carried out at a flow rate of 1.0 mL/min. After washing the bound proteins for 2.0 min with 0.3% TFA, they were eluted with a 60 min linear gradient of increasing acetonitrile (35−70%) in 0.3% TFA. Fractions of 0.5 mL were collected, and a portion of each was removed and counted for radioactivity.

Peptide Mapping of IsoAsp Sites in H2B from Aged Nucleosomes. Histone H2B (500 μg) was isolated by RP-HPLC (described above) from both unaged and 16 day aged rat liver nucleosomes. The nucleosomes used here were not ^{3}H-methylated prior to HPLC. The H2B peak was concentrated to dryness in a vacuum centrifuge, dissolved in 50 mM ammonium acetate, pH 4.0, and digested with endoproteinase Glu-C at a protease:H2B ratio of 1:10 by weight. Digestion was carried out for 20 h at 37 °C and then terminated by the addition of 3,4-dicholoroisocoumarin to a final concentration of 200 μM followed by freezing at −70 °C. Samples were concentrated to dryness, dissolved in 100 μL of water, redried to reduce residual levels of digestion buffer, and finally redissolved in 100 μL of water. Ten microliters of this was ^{3}H-methylated with PIMT to label isoAsp-containing peptides prior to peptide separation by RP-HPLC. Separation was carried out with the same column described above using a linear gradient of 5−50% acetonitrile in 0.3% TFA over 100 min. Fractions of 0.5 mL were collected, and a portion of each fraction was taken to count the radioactivity. Peptides in the remaining 90 μL of the Glu-C digest were chromatographed in a separate but identical HPLC run without prior methylation. The 214 nm peptide peaks in this latter run were identified by MALDI-TOF (matrix-assisted laser desorption ionization−time of flight) mass spectrometry on a Perseptive Biosystems Voyager DE-Pro instrument.

PIMT-Dependent Repair of Aged Nucleosomes. Repair reactions (100 μL each) were carried out in Slide-A-Lyzer MINI dialysis units (Thermo-Pierce; 7 kDa cutoff) containing the following components: 0.31 μg/μL (as protein) nucleosomes, repair buffer (20 mM K-HEPES, pH 7.8, 1.0 mM EGTA, 1.0 mM DTT), 20 μM AdoMet, 1% (v/v) mammalian protease inhibitor cocktail (Sigma catalog no. P-8340), and 6 μM PIMT. The Slide-A-Lyzer units were dialyzed against an external solution of repair buffer containing 20 μM AdoMet for 20 h at 37 °C. Repair reactions were stopped by adding AdoHcy (a PIMT inhibitor) to a final concentration of 5 mM and then dialyzed against fresh repair buffer for 16 h at 30 °C to allow hydrolysis of any remaining succinimides. To estimate the levels of any remaining isoAsp in the histones, the samples were first concentrated 3-fold using Microcon centrifugal filter units (Millipore/Amicon) and then ^{3}H-methylated as described above. The patterns of [^{3}H]methyl incorporation were determined by SDS−PAGE and fluorography.

Protein Determination. Proteins were precipitated with 7% (w/v) trichloroacetic acid and assayed by the method of Lowry et al. (*26*) using bovine serum albumin as a standard.

RESULTS

IsoAsp Formation during in Vitro Aging of Mononucleosomes Purified from Rat Liver and Chicken Erythrocytes. To investigate the specificity of isoAsp formation in histones during *in vitro* aging, we incubated rat and chicken mono-

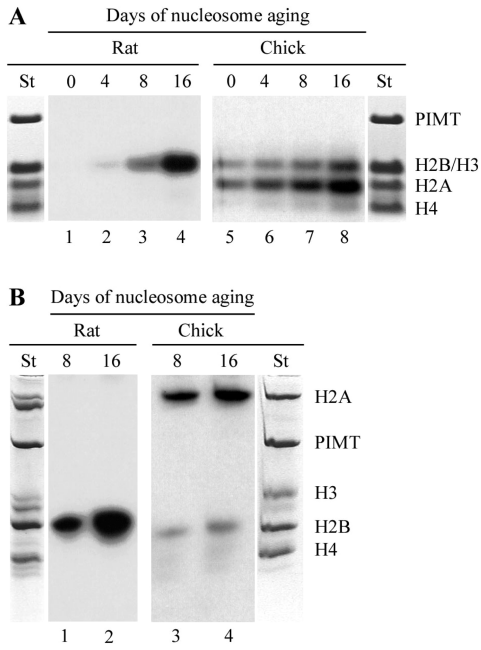

FIGURE 2: Accumulation of isoAsp sites during *in vitro* aging of nucleosomes from rat liver and chicken erythrocytes. Purified rat or chick mononucleosomes were aged *in vitro* for 0−16 days as described in Experimental Procedures and then ^{3}H-methylated by PIMT to radiolabel the isoAsp sites. The resulting patterns of histone methylation were revealed by gel electrophoresis and fluorography. Panel A shows the results of electrophoresis using a modified version of the NuPAGE SDS−PAGE system (Invitrogen) that minimizes loss of the alkaline-labile isoAsp [^{3}H]methyl esters. The lanes labeled "St" on the far left and far right lanes show the Coomassie Blue protein staining patterns of methylation reactions for the unaged rat and chick nucleosomes, respectively. Lanes 1−8 are fluorograms showing the pattern of [^{3}H]methyl incorporation into isoAsp-bearing histones. Panel B shows the results of UAT-PAGE and corresponding fluorograms for the 8 and 16 day aged nucleosomes. The UAT system was employed because it separates histones H2B and H3 well, unlike the NuPAGE system. All lanes in panels A and B contained approximately 4 μg of nucleosomal protein, along with PIMT enzyme that was present in the methylation reaction. Fluorograms were obtained from 3 day exposures.

nucleosomes in a pH 7.4 buffer at 37 °C for 0−16 days. Samples were taken at 4 day intervals to examine isoAsp content by PIMT-catalyzed ^{3}H-methylation. Figure 2 shows the pattern of isoAsp accumulation in core histones after electrophoretic separation and ^{3}H fluorography. In panel A, histone separation was achieved by SDS−PAGE using a modified protocol for the NuPAGE Bis-Tris gel system because the relatively low pH of this system minimizes spontaneous hydrolysis of the isoaspartyl [^{3}H]methyl esters. With rat nucleosomes, isoAsp accumulated exclusively in a band that coincided with histones H2B and H3. With chicken nucleosomes, isoAsp accumulation was seen primarily in histone H2A, with a lesser but significant accumulation also occurring in the H2B/H3 band. Because the NuPAGE system did not separate histones H2B and H3, we reexamined the ^{3}H-methylation pattern using a urea/acetic acid/Triton (UAT) gel system (panel B). With rat nucleosomes, it is clear that isoAsp accumulated only in histone H2B. For chick nucleosomes, the UAT system confirmed the pattern seen in Figure 2A, that is, a predominant accumulation in H2A and a lesser accumulation in H2B.

To determine the actual rates of isoAsp formation in individual histones, aged nucleosomes were evaluated for

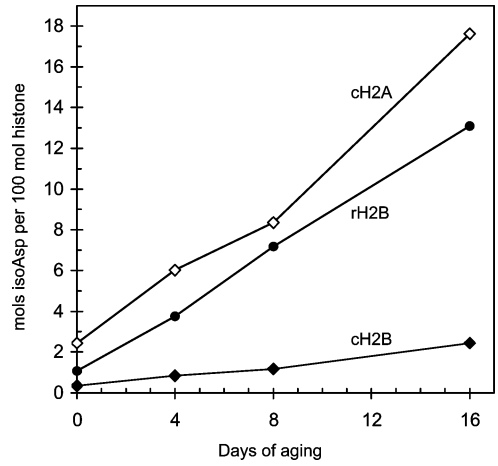

FIGURE 3: Stoichiometry and kinetics of isoAsp formation during *in vitro* aging of nucleosomes from rat liver and chicken erythrocytes. Purified rat or chick mononucleosomes were aged *in vitro* for 0−16 days as in Figure 2, and the total amount of isoAsp in each sample was then determined using the AdoHcy/HPLC assay described in Experimental Procedures. The fraction of total isoAsp attributable to H2A or H2B was then determined by densitometric scanning of the relevant gel lanes in Figure 2 using UN-SCAN-IT gel software (Silk Scientific). Data for chick H2B (◆), rat H2B (●), and chick H2A (◇) are shown.

total isoAsp content by measuring the stoichiometric production of AdoHcy from AdoMet as described in Experimental Procedures. These data were combined with densitometric analysis of the fluorograms seen in Figure 2 to determine the mol % accumulation of isoAsp in the aged nucleosomes (Figure 3). From this graph we estimate that the rates of isoAsp accumulation seen in Figure 2, expressed as mol % per day, are 0.91%, 0.72%, and 0.13% for chicken H2A, rat H2B, and chicken H2B, respectively. It is noteworthy that the rate of isoAsp formation observed in rat liver H2B (0.72% per day) in this experiment is close to our previous estimate of ∼1% per day for isoAsp formation in H2B in cultured rat PC12 cells.

Histone Sequence Differences between Rat and Chicken Support Observed Differences in IsoAsp Accumulation. Several studies on isoAsp formation during *in vitro* aging of synthetic peptides and recombinant proteins indicate that it is strongly influenced by two structural factors: the identity of the amino acid that is C-flanking to the susceptible Asx residue and the local flexibility of the polypeptide in the region containing the susceptible Asx residue. Small hydrophilic residues in the C-flanking position favor isoAsp formation, with glycine and serine being the most frequently observed.

In a previous report on isoAsp formation in rat brain H2B, we suggested that the Asp25−Gly26 bond that lies in the highly flexible N-terminal tail of H2B was the most likely candidate for isoAsp formation among the six total Asx residues in this histone (*10*). In the present work we chose to compare isoAsp formation in nucleosomes from rat and chicken, because in chicken H2B, the α-carboxyl of the homologous aspartate residue (Asp26) is linked to a relatively bulky lysine residue that should greatly slow the rate of isoAsp formation (Figure 4). The results shown in Figures 2 and 3 confirm our prediction; the rate of isoAsp formation in chicken H2B is less than one-fifth that of rat H2B. Outside of the flexible N-terminal tail of H2B, there are no relevant

A H2B: rat (Q6ZWY9) vs. chicken (P0C1H3)

```
r  PEPAKSAPAP KKGSKKAVTK AQKKDGKKRK RSRKESYSVY 40
c  .......... .......... T...GD.... K.......I.

r  VYKVLKQVHP DTGISSKAMG IMNSFVNDIF ERIAGEASRL 80
c  .......... .......... .......... ..........

r  AHYNKRSTIT SREIQTAVRL LLPGELAKHA VSEGTKAVTK 120
c  .......... .......... .......... ..........

r  YTSSK 125
c  .....
```

B H2A: chicken (P02263) vs. rat (P0C169)

```
c  SGRGKQGGKA RAKAKSRSSR AGLQFPVGRV HRLLRKGNYA 40
r  .......... .......... .......... ..........

c  ERVGAGAPVY LAAVLEYLTA EILELAGNAA RDNKKTRIIP 80
r  .......... .......... .......... ..........

c  RHLQLAIRND EELNKLLGKV TIAQGGVLPN IQAVLLPKKT 120
r  .......... ........R. .......... ..........

c  DSH-KAKAK 128
r  E..H...G.
```

FIGURE 4: Sequence comparisons of histones H2A and H2B from rat and chicken. The predicted, and subsequently confirmed, location of the isopeptide bond in rat H2B is marked by the caret symbol. All Asp and Asn residues are underlined. Sequences were obtained from the UniProt Knowledgebase (release 13.4) via the ExPasy Proteomics Server (ca.expasy.org/sprot/). Alignments were carried out with Clustal W (1.83). Accession numbers (common to both the ExPasy and NCBI protein databases) are shown on the first line of parts A and B of this figure. The accession number used for rat H2B is actually for mouse H2B (which has an identical sequence). The sequence of the major somatic isoform of rat H2B has been determined by Martinage et al. (*41*) and is listed in the NCBI protein database under accession number 0506206A and gi 223096.

differences between the rat and chick sequences, adding further strength to the idea that Asp25 in rat H2B is the major source of isoAsp formation in the rat nucleosome.

We did not anticipate the rapid formation of isoAsp seen in chick H2A because the flexible N-terminal tail of chick H2A does not harbor any isoAsp-prone sequences. In considering the entire chick H2A molecule, however, a likely candidate for isoAsp formation emerges at Asp121-Ser122 in the C-terminal tail (Figure 4). H2A is atypical among the four core histones in that it has a relatively large and flexible C-terminal tail that starts at or before Lys119 in the chicken sequence (*27, 28*). In rat, this residue is replaced by a glutamate, which would explain why rat H2A does not accumulate isoAsp.

Confirmation That Asp25 Is the Major Site of IsoAsp Formation in Rat H2B. To directly identify the major site(s) of isoAsp formation in rat nucleosomes, we ^{3}H-methylated rat nucleosomes that were aged for 16 days and then separated the core histones by reversed-phase HPLC. As shown in Figure 5, virtually all of the [^{3}H]methyl label was incorporated into H2B. The same HPLC method was then used to bulk-purify unlabeled H2B from aged rat nucleosomes. The aged H2B was digested with endoproteinase Glu-C, and a portion of the resulting peptide mixture was ^{3}H-methylated prior to separation of the peptides by reversed-phase HPLC. A parallel digestion and HPLC peptide map was also carried out on H2B from unaged nucleosomes to serve as a control. Figure 6 shows a plot of ^{3}H-incorporation for each HPLC fraction of the aged H2B digest after correcting for any ^{3}H-incorporation in the same fraction from the control run. Superimposed over these data is a UV trace of the aged histone peptides. Table 1 summarizes the mass analysis data used to identify the UV peaks. All amino acids in the H2B sequence are accounted for except for residues 72−76, a short peptide that does not contain any Asx residues. The data in Figure 6 show that the major source of isoAsp in aged H2B lies in residues 1−35. Since Asp25 is the only Asx residue in this region, the expectation of this site from sequence and flexibility considerations was confirmed.

PIMT Repairs IsoAsp Sites in Aged Nucleosomes. Previous studies with synthetic peptides and several purified proteins have demonstrated that PIMT catalyzes the repair of atypical L-isoaspartyl peptide bonds by the mechanism shown in Figure 1. To see if PIMT can also repair isoAsp sites in age-damaged nucleosomes, we employed a three-step protocol that has recently been shown to efficiently repair the brain protein synapsin I isolated from PIMT-KO mice (*23*). In step 1 (the actual repair step), a solution of analyte (in this case aged nucleosomes) and recombinant PIMT was dialyzed at pH 7.8 against an excess of unlabeled AdoMet to ensure a constant high ratio of AdoMet to AdoHcy (a product of the methylation reaction and a competitive inhibitor of PIMT). In step 2, dialysis against buffer alone served to remove unlabeled AdoMet and ensure hydrolysis of any residual methyl esters or succinimide intermediates (Figure 1). In step 3, ^{3}H-methylation of the analyte protein with PIMT was carried out at pH 6.4 to radiolabel any unrepaired isoAsp sites. Figure 7 shows the results of a repair experiment carried out with nucleosomes from rat brain (lanes 1−4) and chicken erythrocytes (lanes 5−8) that had been aged for 8 days. The amount of isoAsp H2B in the control (Con) rat nucleosomes (which underwent a mock repair with PIMT omitted in step 1) is shown in lane 1. In contrast, inclusion of PIMT in a complete repair reaction (Rep, lane 2) resulted in the nearly total elimination of isoAsp sites as judged by the low level of [^{3}H]methyl incorporation. A similar result is seen for the repair of both H2A and H2B in chick nucleosomes (lane 6 vs lane 5).

DISCUSSION

Previous studies in this laboratory with cultured rat PC12 cells and a PIMT knockout mouse led to the discovery that histone H2B is a major endogenous substrate for PIMT in the rodent nucleus (*10*). The present study demonstrates that purified nucleosomes aged in a physiological buffer produce the same pattern of histone modification that was observed *in vivo*. This strongly suggests that isoAsp formation in H2B *in vivo* is a self-catalyzed reaction that can occur at the level of the intact nucleosome. The large-scale production of purified nucleosomes allowed us to map the major site of isoAsp formation in rat H2B to the Asp25−Gly26 bond in the highly flexible N-terminal tail. We were also able to demonstrate that recombinant rat PIMT can eliminate nearly all of the isoAsp residues that accumulate during aging of rat and chicken nucleosomes.

The accumulation of isoAsp in histone H2B may contribute to the phenotype of the PIMT-KO mouse and potentially

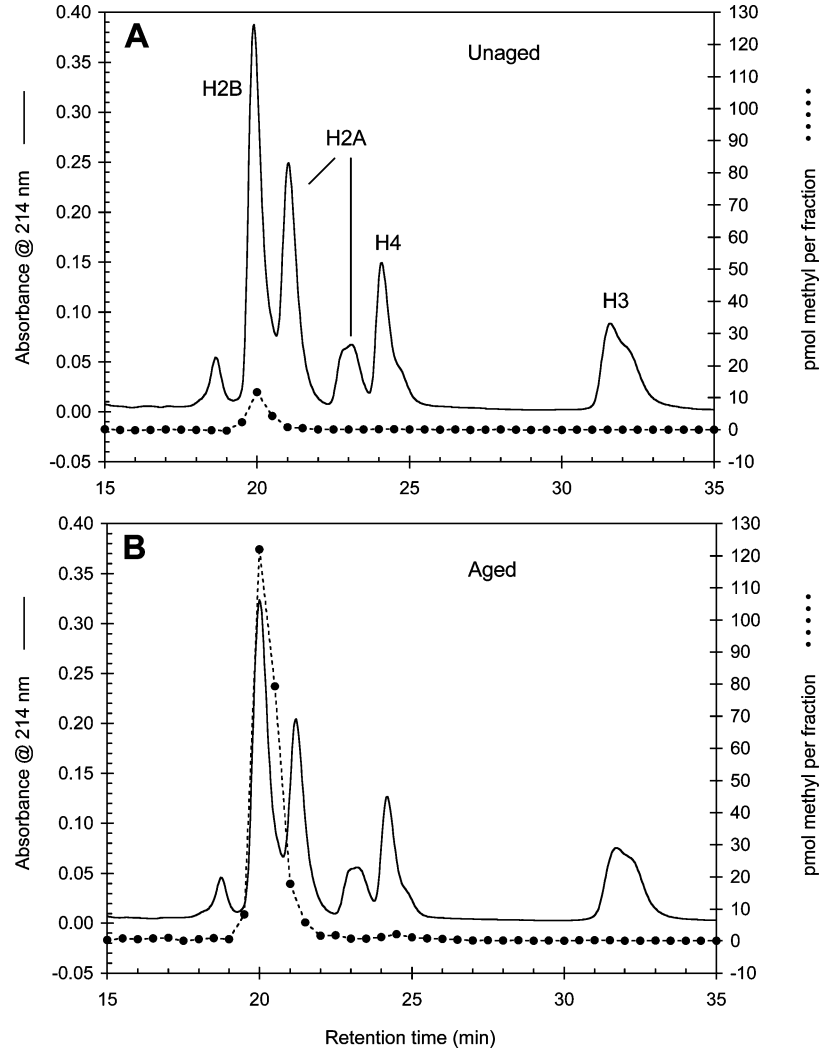

FIGURE 5: Purification and methyl-acceptor activity of core histones isolated from rat liver. Rat liver nucleosomes that were unaged (panel A) or aged (panel B) *in vitro* for 16 days were ^{3}H-methylated by PIMT and then separated by reversed-phase HPLC. Histone peaks were identified by SDS−PAGE relative to commerical histone standards from calf thymus.

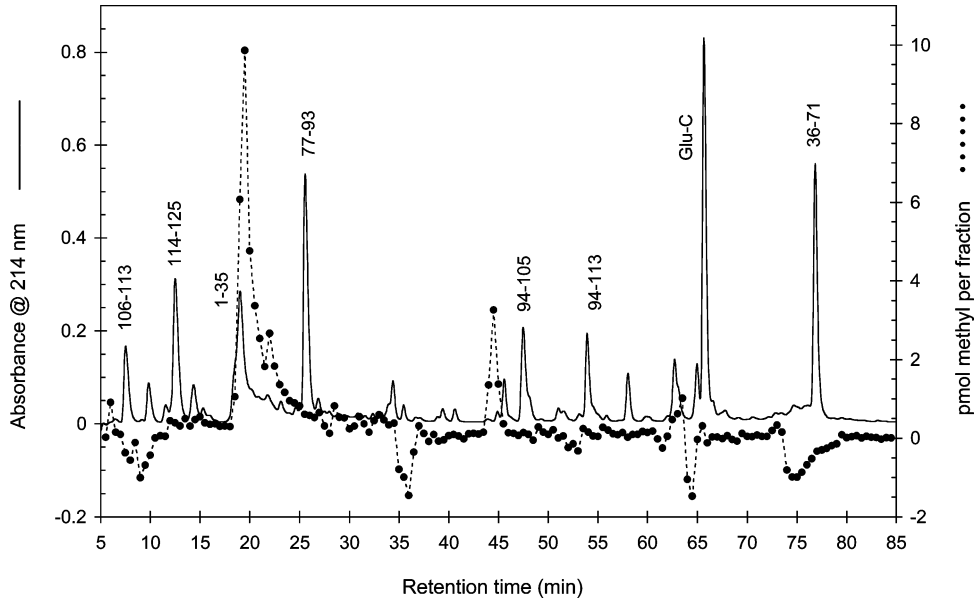

FIGURE 6: Determination of the major methyl-accepting (isoAsp-bearing) site in histone H2B from aged rat liver nucleosomes. H2B was purified from aged (16 day) rat liver nucleosomes by reversed-phase HPLC. After digestion with endoproteinase Glu-C, the resulting H2B peptides were separated into two fractions. One fraction (10% of the total) was ^{3}H-methylated with PIMT to radiolabel the isoAsp peptide(s) that were then separated by RP-HPLC. The remaining 90% was taken directly for RP-HPLC in a parallel run to establish the retention times and identities of the Glu-C-generated peptides. The peptides from this latter run were identified by mass spectrometry (Table 1).

Table 1: Identification by MALDI-TOF Mass Spectrometry of Rat H2B Peptides Shown in Figure 6

peptide	retention time (min)	obsd av mass (Da)	expected av mass[a] (Da)	Δ (Da)
1−35	19.1	3846.49	3846.59	−0.10
36−71	76.9	4069.08	4069.72	−0.64
72−76[b]			545.62	
77−93	25.6	1990.99	1991.23	−0.22
94−105	47.5	1310.74	1310.59	+0.15
94−113	53.9	2146.82	2146.55	+0.27
106−113	7.6	855.01	854.99	+0.02
114−125	12.5	1271.03	1271.47	−0.44

[a] Expected masses were obtained by *in silico* digestion (endoproteinase Glu-C in bicarbonate buffer) of the rat sequence shown in Figure 4 using the Peptide Mass program at http://ch.expasy.org/tools/peptide-mass.html. [b] This peptide was not found.

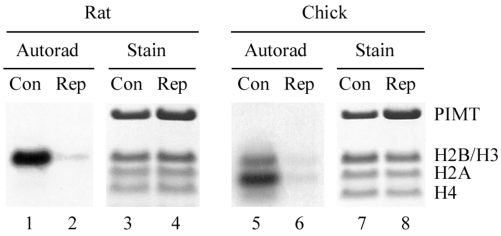

FIGURE 7: PIMT catalyzes repair of isoAsp sites in age-damaged nucleosomes. Rat or chick nucleosomes that had been aged for 8 days were incubated for 20 h with PIMT and unlabeled AdoMet (as described in Experimental Procedures) in an attempt to repair the isoAsp sites. The repaired samples were dialyzed overnight to remove unlabeled AdoMet and allow for complete hydrolysis of the succinimide intermediates that form during the repair cycle (Figure 1). The samples were then assessed for remaining isoAsp content in a standard ^{3}H-methylation assay. Odd numbered lanes (labeled Con) are control samples in which no PIMT was present during the repair reaction. Even numbered lanes (labeled Rep) did contain PIMT in the repair reaction. IsoAsp content, as measured by ^{3}H-methylation capacity, is shown in lanes 1 and 2 for the rat nucleosomes and in lanes 5 and 6 for the chick nucleosomes. As expected, lanes 1 and 5 of this figure show the same pattern of [^{3}H]methyl incorporation as do lanes 3 and 7, respectively, of Figure 2A. The greatly reduced ^{3}H-methylation seen in lanes 2 and 6 indicates that substantial repair of isoAsp sites occurs in both rat and chick nucleosomes when PIMT is present in the repair reaction.

to any human neurological disease where PIMT function is compromised. PIMT knockout mice exhibit altered metabolic pathways (*29, 30*), hyperresponsive CD4(+) T cells (*31*), cognitive deficits, atypical behavior, and neuronal pathology and pathophysiology (*32*−*35*) and typically succumb to fatal epileptic seizures between 30 and 90 days after birth (*8, 9*). Isomerization of the Asp25−Gly26 bond could alter the interaction of H2B with the surrounding DNA, alter the interaction of the tail with transcriptional coactivators, or alter the susceptibility of nearby residues such as Lys23, a known acetylation site (*36*), to modification by histone acetyltransferases. Thus, a PIMT deficiency could compromise normal cell function not only by failing to repair a host of damaged cellular proteins but also by altering normal patterns of gene expression.

The susceptibility of histone H2B to succinimide formation also has potentially important implications in cells where PIMT activity is normal. It was recently shown that approximately 12% of Asp25 in histone H2B of normal mice is present as the D-enantiomer (*37*). This arises as the result of a slow racemization that occurs each time a susceptible Asx−X bond passes through the succinimide form (*38*−*40*). As predicted by the repair pathway in Figure 1, the rate of Asp25 racemization *in vivo* is ironically accelerated by the presence of PIMT. The D-enantiomer is most likely a mixture of D-isoAsp and D-Asp, both of which could significantly alter H2B function for the same reasons suggested above for the L-isoaspartyl form. The "histone code" entails several distinct types of side-chain modification that include acetylation, methylation, and ubiquitination of lysine residues and phosphorylation of serine residues. In bulk-isolated histones, the stoichiometry of modification at any given residue is usually well below 5% (*36*), reflecting the heterogeneity of chromatin microstructure and gene status. It remains to be determined if the isomerization/racemization-prone nature of the Asp25−Gly26 bond in mammalian H2B is silent and ignored or whether it plays some cryptic role in regulating chromatin function.

ACKNOWLEDGMENT

We thank Kate Reissner for advice on design of the repair reaction, Brandon Schurter for help and advice with operation of the HPLC and mass spectrometry equipment, and Cynthia David for general assistance and advice throughout this project.

REFERENCES

1. Volkin, D. B., Mach, H., and Mudbug, C. R. (1997) Degradative covalent reactions important to protein stability. *Mol. Biotechnol. 8*, 105–122.
2. Reissner, K. J., and Aswad, D. W. (2003) Deamidation and isoaspartate formation in proteins: unwanted alterations or surreptitious signals? *Cell. Mol. Life Sci. 60*, 1281–1295.
3. Clarke, S. (2003) Aging as war between chemical and biochemical processes: protein methylation and the recognition of age-damaged proteins for repair. *Ageing Res. Rev. 2*, 263–285.
4. Zhu, J. X., Doyle, H. A., Mamula, M. J., and Aswad, D. W. (2006) Protein repair in the brain, proteomic analysis of endogenous substrates for protein L-isoaspartyl methyltransferase in mouse brain. *J. Biol. Chem. 281*, 33802–33813.
5. Wakankar, A. A., Borchardt, R. T., Eigenbrot, C., Shia, S., Wang, Y. J., Shire, S. J., and Liu, J. L. (2007) Aspartate isomerization in the complementarity-determining regions of two closely related monoclonal antibodies. *Biochemistry 46*, 1534–1544.
6. Vigneswara, V., Lowenson, J. D., Powell, C. D., Thakur, M., Bailey, K., Clarke, S., Ray, D. E., and Carter, W. G. (2006) Proteomic identification of novel substrates of a protein isoaspartyl methyltransferase repair enzyme. *J. Biol. Chem. 281*, 32619–32629.
7. Johnson, B. A., Najbauer, J., and Aswad, D. W. (1993) Accumulation of substrates for protein L-isoaspartyl methyltransferase in adenosine dialdehyde-treated PC12 cells. *J. Biol. Chem. 268*, 6174–6181.
8. Kim, E., Lowenson, J. D., MacLaren, D. C., Clarke, S., and Young, S. G. (1997) Deficiency of a protein-repair enzyme results in the accumulation of altered proteins, retardation of growth, and fatal seizures in mice. *Proc. Natl. Acad. Sci. U.S.A. 94*, 6132–6137.
9. Yamamoto, A., Takagi, H., Kitamura, D., Tatsuoka, H., Nakano, H., Kawano, H., Kuroyanagi, H., Yahagi, Y., Kobayashi, S., Koizumi, K., Sakai, T., Saito, K., Chiba, T., Kawamura, K., Suzuki, K., Watanabe, T., Mori, H., and Shirasawa, T. (1998) Deficiency in protein L-isoaspartyl methyltransferase results in a fatal progressive epilepsy. *J. Neurosci. 18*, 2063–2074.
10. Young, A. L., Carter, W. G., Doyle, H. A., Mamula, M. J., and Aswad, D. W. (2001) Structural integrity of histone H2B in vivo requires the activity of protein L-isoaspartyl O-methyltransferase, a putative repair enzyme. *J. Biol. Chem. 276*, 37161–37165.
11. Clarke, S. (1987) Propensity for spontaneous succinimide formation from aspartyl and asparaginyl residues in cellular proteins. *Int. J. Pept. Protein Res 30*, 808–821.
12. Brennan, T. V., and Clarke, S. (1995) Deamidation and isoaspartate formation in model synthetic peptides: the effects of sequence and solution environment, in *Deamidation and Isoaspartate Formation*

in Peptides and Proteins (Aswad, D. W., Ed.) pp 65−90, CRC Press, Boca Raton, FL.
13. Kossiakoff, A. A. (1988) Tertiary structure is a principal determinant to protein deamidation. *Science 240*, 191–194.
14. Johnson, B. A., and Aswad, D. W. (1995) Deamidation and isoaspartate formation during in vitro aging of purified proteins, in *Deamidation and Isoaspartate Formation in Peptides and Proteins* (Aswad, D. W., Ed.) pp 91−113, CRC Press, Boca Raton, FL.
15. Robinson, N. E., Robinson, Z. W., Robinson, B. R., Robinson, A. L., Robinson, J. A., Robinson, M. L., and Robinson, A. B. (2004) Structure-dependent nonenzymatic deamidation of glutaminyl and asparaginyl pentapeptides. *J. Pept. Res. 63*, 426–436.
16. Chirpich, T. P. (1968) Lysine 2,3-aminomutase; Purification and Properties, Ph.D. Thesis, University of California, Berkeley.
17. David, C. L., and Aswad, D. W. (1995) Cloning, expression, and purification of rat brain protein L-isoaspartyl methyltransferase. *Protein Expression Purif. 6*, 312–318.
18. Hewish, D. R., and Burgoyne, L. A. (1973) Chromatin substructure. The digestion of chromatin DNA at regularly spaced sites by a nuclear deoxyribonuclease. *Biochem. Biophys. Res. Commun. 52*, 504–510.
19. Weintraub, H., Palter, K., and Van Lente, F. (1975) Histones H2a, H2b, H3, and H4 form a tetrameric complex in solutions of high salt. *Cell 6*, 85–110.
20. Thomas, J. O. (1998) Isolation and fractionation of chromatin and linker histones, in *Chromatin: a practical approach* (Gould, H., Ed.) pp 1−34, Oxford University Press, New York.
21. Schurter, B. T., and Aswad, D. W. (2000) Analysis of isoaspartate in peptides and proteins without the use of radioisotopes. *Anal. Biochem. 282*, 227–231.
22. Laemmli, U. K., and Favre, M. (1973) Maturation of the head of bacteriophage T4. *J. Mol. Biol. 80*, 575–599.
23. Reissner, K. J., Paranandi, M. V., Luc, T. M., Doyle, H. A., Mamula, M. J., Lowenson, J. D., and Aswad, D. W. (2006) Synapsin I is a major endogenous substrate for protein L-isoaspartyl methyltransferase in mammalian brain. *J. Biol. Chem. 281*, 8389–8398.
24. Chamberlain, J. P. (1979) Fluorographic detection of radioactivity in polyacrylamide gels with the water-soluble fluor, sodium salicylate. *Anal. Biochem. 98*, 132–135.
25. Weikowski, M., and DePamphilis, M. L. (1993) One-dimensional gel analysis of histone synthesis. *Methods Enzymol. 225*, 489–501.
26. Lowry, O. H., Rosebrough, N. J., Farr, A. L., and Randall, R. J. (1951) Protein measurement with the Folin phenol reagent. *J. Biol. Chem. 193*, 265–275.
27. Usachenko, S. I., Bavykin, S. G., Gavin, I. M., and Bradbury, E. M. (1994) Rearrangement of the histone H2A C-terminal domain in the nucleosome. *Proc. Natl. Acad. Sci. U.S.A. 91*, 6845–6849.
28. Luger, K., Mäder, A. W., Richmond, R. K., Sargent, D. F., and Richmond, T. J. (1997) Crystal structure of the nucleosome core particle at 2.8 Å resolution. *Nature 389*, 251–260.
29. Farrar, C., and Clarke, S. (2002) Altered levels of S-adenosylmethionine and S-adenosylhomocysteine in the brains of L-isoaspartyl (D-aspartyl) O-methyltransferase-deficient mice. *J. Biol. Chem. 277*, 27856–27863.
30. Farrar, C., Houser, C. R., and Clarke, S. (2005) Activation of the PI3K/Akt signal transduction pathway and increased levels of insulin receptor in protein repair-deficient mice. *Aging Cell 4*, 1–12.
31. Doyle, H. A., Gee, R. J., and Mamula, M. J. (2003) A failure to repair self-proteins leads to T cell hyperproliferation and autoantibody production. *J. Immunol. 171*, 2840–2847.
32. Kim, E., Lowenson, J. D., Clarke, S., and Young, S. G. (1999) Phenotypic analysis of seizure-prone mice lacking L-isoaspartate (D-aspartate) O-methyltransferase. *J. Biol. Chem. 274*, 20671–20678.
33. Ikegaya, Y., Yamada, M., Fukuda, T., Kuroyanagi, H., Shirasawa, T., and Nishiyama, N. (2001) Aberrant synaptic transmission in the hippocampal CA3 region and cognitive deterioration in protein-repair enzyme-deficient mice. *Hippocampus 11*, 287–298.
34. Vitali, R., and Clarke, S. (2004) Improved rotorod performance and hyperactivity in mice deficient in a protein repair methyltransferase. *Behav. Brain Res. 153*, 129–141.
35. Farrar, C. E., Huang, C. S., Clarke, S. G., and Houser, C. R. (2005) Increased cell proliferation and granule cell number in the dentate gyrus of protein repair-deficient mice. *J. Comp. Neurol. 493*, 524–537.
36. Kim, S. C., Sprung, R., Chen, Y., Xu, Y., Ball, H., Pei, J., Cheng, T., Kho, Y., Xiao, H., Xiao, L., Grishin, N. V., White, M., Yang, X. J., and Zhao, Y. (2006) Substrate and functional diversity of lysine acetylation revealed by a proteomics survey. *Mol. Cell 23*, 607–618.
37. Young, G. W., Hoofring, S. A., Mamula, M. J., Doyle, H. A., Bunick, G. J., Hu, Y., and Aswad, D. W. (2005) Protein L-isoaspartyl methyltransferase catalyzes in vivo racemization of aspartate-25 in mammalian histone H2B. *J. Biol. Chem. 280*, 26094–26098.
38. McFadden, P. N., and Clarke, S. (1987) Conversion of isoaspartyl peptides to normal peptides: Implications for the cellular repair of damaged proteins. *Proc. Natl. Acad. Sci. U.S.A. 84*, 2595–2599.
39. Johnson, B. A., Murray, E. D., Jr., Clarke, S., Glass, D. B., and Aswad, D. W. (1987) Protein carboxyl methyltransferase facilitates conversion of atypical L-isoaspartyl peptides to normal L-aspartyl peptides. *J. Biol. Chem. 262*, 5622–5629.
40. Kinzel, V., Koenig, N., Pipkorn, R., Bossemeyer, D., and Lehmann, W. D. (2000) The amino terminus of PKA catalytic subunit: A site for introduction of posttranslational heterogeneities by deamidation: D-Asp2 and D-isoAsp2 containing isozymes. *Protein Sci. 9*, 2269–2277.
41. Martinage, A., Mangeat, P., Sautiere, P., Marchis-Mouren, G., and Biserte, G. (1979) Amino acid sequence of rat thymus histone H2B and identification of the in vitro phosphorylation sites. *Biochimie 61*, 61–69.

BI8013467